Local atomic structure of CdTe:In at high In concentrations

F. J. Espinosa and J. Mustre de Leon
Cinvestav, Unidad Merida, Merida, Yucatan 97310, Mexico

S. D. Conradson
Los Alamos National Laboratory, Los Alamos, New Mexico 87545

J. L. Peña and M. Zapata-Torres*
Cinvestav, Unidad Merida, Merida, Yucatan 97310, Mexico
(Received 8 September 1999)

The local atomic structure of CdTe:In at In concentrations of 0, 0.5, and 6 at. % was investigated using *x*-ray absorption spectroscopy. Changes in the x-ray-absorption near-edge structure (XANES) and the x-ray-absorption fine structure (XAFS) were detected for the In *K* edge. In the In XANES region, the 0.5 at. % sample exhibits a higher amplitude of the white line than the 6 at. % sample. While in the In *K*-edge XAFS of both samples only the first shell contribution is apparent; the environment around In in the 0.5 at. % sample shows larger disorder than in the 6 at. % In sample. From Cd and Te XAFS the data exhibit the first three shells of neighbors in agreement with the zinc-blende structure of CdTe, showing increased disorder as a function of In concentration. Results from fits and simulations of both XAFS and XANES indicate the formation of *A* centers in the 0.5 at. % sample. For the 6 at. % sample the results indicate a smaller amount of *A* centers. The possibility of *DX* center formation is discussed.

I. INTRODUCTION

The understanding of the doping limit in semiconductors has been a long-standing problem.[1] The mechanisms proposed to limit the incorporation of free carriers with increasing dopant concentration are (i) solubility limits of the dopant, (ii) the presence of native point defects, either isolated or in complexes, and (iii) the presence of local centers which involve large lattice relaxations. Depending on the host system and the dopant any of these mechanisms can be relevant. In order to asses the role of these mechanisms it is necessary to correlate electrical and optical spectroscopical information with structural information.[2–5] Consequently, the local atomic structure of these materials, which is sensitive to the presence of defects and local centers, has received recent attention.

If the solubility limit is exceeded in an attempt to heavily dope the semiconductor, second phases or impurity precipitates appear. Diffraction studies can show the formation of second phases.[6] However, for some compounds the appearance of second phases, as seen in diffraction, occurs at much higher doping levels compared to those in which carrier passivation appears. Hence, it seems an unviable candidate to explain the limits of doping in those systems. The formation of native point defects and complexes can also explain doping limits. Indeed, in II-VI semiconductors, especially with a wide band gap, explanations of doping limits emphasize the role of vacancies either isolated or as part of a complex.[1] The rapid change in the lattice parameter with dopant concentration has been used to signal the presence of these point defects.[7,8] Although spontaneous formation of isolated vacancies with doping could explain carrier passivation, experimental results in II-VI compounds indicate the existence of complexes.[1] In CdTe:In, above a certain dopant level, the spontaneous formation of *A* centers with a substitutional In

(In_{Cd}) and a cation vacancy (V_{Cd}) in the nearest cation site can become energetically favorable, explaining the doping limit in this compound. It is important to note, however, that in some of the II-VI semiconductors and alloys, the observation of persistent conductivity (PPC) and persistent electron paramagnetic resonance (PEPR) suggests that large lattice relaxations, which do not necesarily include a vacancy, would be relevant in carrier passivation.[10–13] The introduction of dopants above a threshold level can generate *DX* centers with large lattice relaxation.[2] For CdTe:In total energy *ab initio* calculations predict the formation of *DX* centers at ~40 meV above the conduction-band minimum.[2] The maximum carrier concentration achieved for CdTe:In is ~10^{18}. This value is consistent with the estimation of the threshold energy of formation of *DX* centers, suggesting that the formation of this defect could be also relevant as a mechanism to limit the doping of this system. In this model for a DX center, a bond between the In impurity and a Te host breaks, displacing the impurity atom by 1.89 Å towards the $[\bar{1},\bar{1},\bar{1}]$ direction, concurrent with the trapping of two carriers. Experimentally, the existence of *DX*-like centers in CdTe:In has been inferred from conductivity experiments under hydrostatic pressure[14] and with alloying with Zn ($Cd_{0.8}Zn_{0.2}$Te:In).[10] In these eperiments, the role of pressure or alloying is to raise the conduction-band minimum in an absolute scale which makes the *DX* center lie in the band gap.

There are, however, few experimental techniques that can probe the microscopic structure around dopants helping to evaluate the importance of the mechanisms mentioned above in a specific system, and validate theoretical models. XAS spectroscopy has proven a useful technique to characterize the local atomic environment around defects in crystalline systems and lattice distortions in semiconductors.[5,8,9,15,16] It
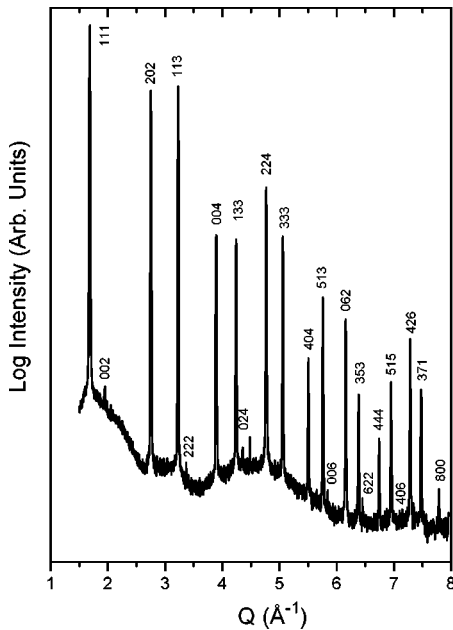
PRB <u>61</u>   7428

FIG. 1. Transmission x-ray-diffraction spectra of the 6 at. % In sample. Indexes of the Bragg peaks are shown confirming the presence of a single-cubic-crystalline phase.

can provide quantitative information about the near-neighbor environment of a particular absorbing atom.[17] Consequently, we have carried x-ray-absorption experiments in CdTe:In samples, with In concentrations of 0, 0.5, and 6 at. %.

II. EXPERIMENTAL PROCEDURE

Samples were prepared using close-spaced vapor transport combined with free evaporation (CSVT-FE) at a base pressure of 10^{-7} Torr.[18,19] The raw materials were CdTe powder 99.999 at. % and indium 99.999 at. % purity from CERAC and Balzers, respectively. Corning 7059 glass slides were used as substrate. The CdTe source was maintained at 600 °C during the growth procedure while the In source temperature was varied between 550 and 700 °C to achieve different concentrations. The temperature of the substrate was fixed at 400 °C. Details of the growth technique can be found elsewhere.[19] It is important to note that for the correct interpretation of structural results the determination of the dopant concentration, rather than the free carrier concentration, is crucial. Elemental concentrations were determined by energy dispersive x-ray spectroscopy using a Jeol 35C electron microscope. X-ray-diffraction (XRD) measurements were performed with a Siemens D5000 diffractometer fitted with a Cu anode. The lattice parameter decreased with the concentration of In in accordance with Ref. 8. A sample of 0.5 at. % In and a sample of 6 at. % In, together with an intrinsic sample were chosen for the study. In order to discard second phase formation as a mechanism for carrier passivation in this system, a transmission XRD experiment at an incident x-ray energy of 26 KeV was performed at the Stanford Synchrotron Radiation Laboratory (SSRL) beamline 7-2 in the 6 at. % In sample. The sample was mounted with the substrate facing the x-ray beam and the sample facing the detector. This confirmed the only presence of the cubic phase. The indexed XRD spectra is shown in Fig. 1 as a function of the

momentum transfer, $Q = 4\pi \sin(\theta)/\lambda$. We chose a logarithmic plot in order to make more visible the possible presence of second phases. We note the smooth varying background due to the presence of the amorphous glass substrate. In this scale the peaks associated with the difference between atomic number of Te and Cd are also visible (e.g., peaks 002, 222, etc.).

X-ray-absorption fine-structure (XAFS) samples were prepared by grinding the shaved film with sucrose and pressing the powder into an aluminum holder sealed in the front and back by kapton tape. The holder was then attached to the cold finger of a cryostat. XAS spectra of In, Cd, and Te of the choosen samples were measured at the Stanford Synchrotron Radiation Laboratory (SSRL) beamline 4-1. Si(220) crystals were used to monochromatize the x-ray beam. Harmonic rejection was accomplished by changing the relative alignment of the two crystals to reduce the flux to 50 % of its maximum level. The data were taken in transmission and fluorescence mode using a 13 element Ge detector for the fluorescence measurements. The signal from 11 of these elements was averaged to obtain a scan in fluorescence mode. A total of three scans were done for the 6 at. % sample and eight scans for the 0.5 at. % due to the small signal from the In fluorescence. We note that Cd fluorescence overlaps with the In fluorescence making the measurement of samples with smaller In concentrations extremely time consuming. Two scans were done for the K-edge XAFS spectra of Cd and Te.

The reduction of the XAFS data was performed using standard procedures.[17] Energy calibration was accomplished by defining the first inflection point in the spectrum of the Cd K edge and Te K edge from undoped CdTe as 26 711 and 31 814 eV, respectively. For In, the first inflection point of the K-edge absorption spectra of an In foil was used as an energy reference at 27 940 eV. E_0 was set equal to the calibration energy such that the photoelectron momentum is $k = \sqrt{(2m/\hbar^2)(E - E_0)}$. The data were normalized by setting the value of a second-order polynomial fit over the pre-edge to zero and a third-order polynomial over the region obove the edge, setting the difference at E_0 to unity. The XAFS were extracted from the spectra as the difference between the normalized spectra and an adjustable spline function over the region above the edge. The parameters of this spline were determined by minimizing the low-frequency residuals (R $\leqslant 1.2$ Å) in the Fourier transform of each absorption spectra.

III. RESULTS

From the normalized absorption spectra of In [Fig. 2(a)], we observe a higher amplitude of the white line of the 0.5 at. % sample than of the 6 at. % sample. This is indicative of a larger amount of unoccupied electronic states with p symmetry with respect to In. This result can be interpreted as arising from having more ionized In atoms in the 0.5 at. % sample. From the normalized absorption spectra of Cd and Te [Figs. 2(b) and 2(c)], changes are smaller and its interpretation is more complex. However, both of them are indicative of changes in the local electronic structure around Cd and Te produced by the introduction of In. Changes in the XAFS are best illustrated in the Fourier-transform magnitude (FTM). In the case of In [Fig. 3(a)], we observe an increase
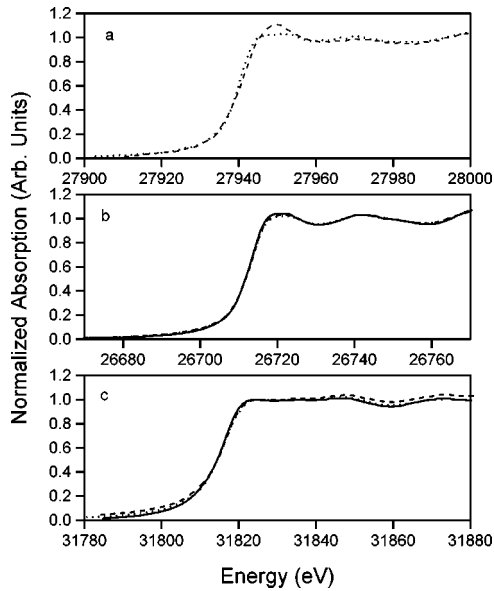
FIG. 2. Absorption edge (K) for the undoped sample (solid line), the 0.5 at. % In sample (dashed line), and the 6 at. % sample (dotted line), of (a) In, (b) Cd, and (c) Te.

in the amplitude in the 6 at. % sample with respect to the 0.5 at. % sample. This is counterintuitive since the data are normalized in a per atom basis. This indicates that at 0.5 at. % In, the In atoms are more disordered or less coordinated than at 6 at. % In, if the normal assumption of a Gaussian distribution of neighbors is used. In both In FTM's, we cannot observe contributions from shells beyond the nearest-neighbor shell. This behavior is characteristic of amorphus materials. However, XRD data show that both samples are crystalline. Hence, this behavior could originate from having In in different neighbor environments leading to a very broad
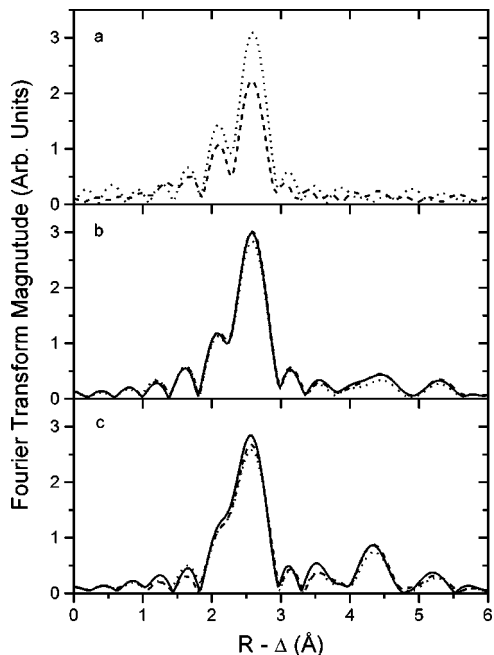

FIG. 3. Fourier-transform magnitude of the XAFS of the undoped sample (solid line), the 0.5 at. % In sample (dashed line), and the 6 at. % sample (dotted line) of (a) In, (b) Cd, and (c) Te.

distribution of farther out shells. For the Cd K edge [Fig. 3(b)] we observe a slight decrease in the amplitude of the main peak for the 6 at. % sample, in consistency with results of Ref. 8. Also, we observe peaks associated up to third neighbors in the crystal structure in all, doped and undoped samples. For the Te K edge [Fig. 3(c)], a small decrease in the amplitude of the main peak is also observed as a function of In concentration. For both Cd and Te, the decrease in amplitude of the main peak correlates with the increase in In content consistent with an increase in the static disorder of the material caused by the introduction of In.

Quantitative information was obtained fitting the XAFS spectra in k space, over the region $2.6 \leq k \leq 13.4$ Å^{-1}. For the In XAFS fit, the distance to neighbors (R), the Debye-Waller factor (σ), and the number of neighbors (N), were left as floating parameters. E_0 was set to 6.1 eV and the overall scale factor S_0^2 was set to 1.05. For Cd the number of neighbors was fixed to the crystallographic value of CdTe, E_0 was set to 5.03 eV, and S_0^2 was set to 0.94. For Te, the number of neighbors was also fixed to the crystallographic value, E_0 was set to 5.2 eV, and S_0^2 was set to 0.92. The photoelectron scattering factors were obtained from the program FEFF.[20] Uncertainties in the reported quantities were obtained by comparing fits to the average spectra to fits done on individual scans or by finding the change in a given parameter which would yield to a 10 % decrease in the quality of the fit. The reported uncertainties correspond to the larger of these estimates.[21] The results of the fits are shown in Table I. Consistent with qualitative results, for In, we obtained a fit that reproduced the spectra using only the first shell of neighbors. The change in the amplitude between the 0.5 at. % and the 6 at. % is reflected mainly in σ. From the Cd and Te XAFS we can identify the first three shells of neighbors; however, changes in the structural parameters of these shells are within experimental uncertanties. The distances of these shells are in agreement with the zinc-blende structure of CdTe.[22]

Although the formulation of a detailed model for the incorporation of In in CdTe at these levels of impurification would require structural probes at a mesoscopic scale (6 to 50 Å), we can check consistency of proposed models of defects. We modeled the In K-edge XAFS using the *ab initio* code FEFF7 which has shown reliable results in this system.[8,20] In Fig. 4(a) we show the overlay of various simulations. The A center was simulated with an In atom in the substitutional Cd site with an In-Te distance of 2.79 Å, which is the In-Te distance obtained from our fits (and its close to the ideal crystallographic distance of 2.80 Å) and a vacancy in one of the Cd atoms in the second-neighbor shell. The absence of one of the 12 second-neighbor shell atoms would generate only a minor reduction of the second shell amplitude. However, the introduction of a lattice relaxation towards the vacancy influences the amplitude and phases of the XAFS oscillations. We simulated a relaxation allowing the Te atoms neighboring the vacancy (one of them is the dopant nearest neighbor) to relax towards the vacancy by 0.26 Å. This relaxation was chosen to explain the rapid decrease of the lattice parameter observed in these kind of samples.[23] This produces a notorious reduction in the amplitude of the first shell of neighbors; however, the amplitude of the next-neighboring shells changes in a much smaller pro-

TABLE I. Results of the fits to the XAFS indicating the distance (R), number of neighbors (N), and the Debye-Waller factor (σ) for the first three shells of neighbors of Cd, Te, and In for undoped, 0.5 at. %, and 6 at. % In impurified samples.

	Cd (0 %)	Cd (0.5 %)	Cd (6 %)	Te (0 %)	Te (0.5 %)	Te (6 %)	In (0.5 %)	In (6 %)
R (Å)	2.79 (1)	2.79 (1)	2.79 (1)	2.78 (1)	2.79 (1)	2.79 (1)	2.78 (1)	2.79 (1)
N	4	4	4	4	4	4	3.9 (4)	3.8 (4)
σ (Å)	0.049 (10)	0.048 (10)	0.054 (9)	0.050 (8)	0.054 (8)	0.055 (8)	0.083 (12)	0.056 (10)
R (Å)	4.56 (2)	4.57 (2)	4.57 (2)	4.55 (2)	4.55 (2)	4.55 (2)		
N	12	12	12	12	12	12		
σ (Å)	0.107 (14)	0.105 (12)	0.117 (15)	0.093 (9)	0.092 (9)	0.098 (10)		
R (Å)	5.31 (3)	5.33 (3)	5.32 (3)	5.33 (2)	5.33 (2)	5.33 (2)		
N	12	12	12	12	12	12		
σ (Å)	0.117 (15)	0.112 (15)	0.121 (15)	0.104 (11)	0.113 (12)	0.115 (12)		

portion. The DX center was simulated as functionally described in Ref. 2, displacing the In atom by 1.89 Å towards the $[\bar{1},\bar{1},\bar{1}]$ direction. The In-Te distances were taken from our fits to the data (2.79 Å). Since in this center one In atom needs to be in the substitutional position In_{Cd} to give up an electron to form a relaxed DX center at another In atom, with the capture of two electrons, the simulation averaged the spectra from a relaxed In and a substitutional In. In these simulations we have used Debye-Waller factors obtained from the fits to the Cd and Te K edges. We used these factors instead of those that can be obtained from a Debye-correlated model, since such a model is known to underestimate the Debye-Waller factors for farther out shells. We also simulated the x-ray-absorption near-edge structure (XANES), with the structural models described above, using a full multiple-scattering calculation with spherically symmetric self-consistent scattering potentials, using the program of Ref. 24 in a cluster of 50 atoms centered around an In atom. The results of the simulations are shown in Fig.

FIG. 4. (a) Fourier-transform magnitude of In XAFS, and (b) absorption-edge simulations for sustitutional In (solid line), In in an A center (dashed line), and In in a DX center (dotted line).

4(b). The observed trend indicates a reduction in the white line amplitude as we go from the ideal substitutional In to the A center and finally to the DX center. To interpret these changes we calculated the projected angular momentum local density of states around In in the presence of a core hole induced by the x-ray-absorption process. The main change in the spectrum is a change in the density of p states of the In, although there are also changes in s and d states not reflected in the K-edge absorption.

The simulations suggest that the 0.5 at. % In sample contains A centers yielding the observed reduced amplitude of the main peak in the XAFS FTM. The increased amplitude of the main peak of the XAFS FTM in the 6 at. % In sample, as compared to the 0.5 at. % sample, would indicate a reduction in the number of of A centers. Furthermore, the reduced amplitude of the white line in the XANES of the 6 at. % sample indicates charge localization around the dopant, filling empty p states. This is consistent with carrier trapping occurring at the dopant site, as it is the case for DX centers. The DX center XAFS simulation shows a small decrease in the first shell amplitude and a large decrease in farther out shells. This is caused by the multiple neighbor environment that this center produces for farther out shells. The increase in the first shell amplitude in the In FTM and the behavior of the white line of the XANES of In support the DX-center formation. However, a different approach (e.g., measurements with photoexcitation) in the measurement is necessary in order to fully test this possibility. Such measurements have been reported elsewhere.[25]
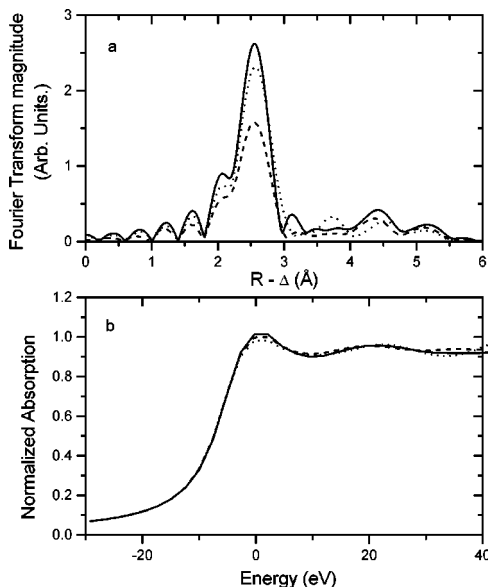
IV. SUMMARY

In this work we have used techniques that provide atomic structural information to understand the microscopic basis for carrier passivation in the CdTe:In system. From our x-ray-diffraction results we conclude that phase separation is not relevant as a limiting doping mechanism. Such a result is expected given the similar ionic radii of Cd and In atoms. We note, however, that diffraction results do not yield direct information about defect structure and x-ray absorption yields more detailed information. The combination of qualitative results, quantitative results, and simulations indicates that for concentrations of $\simeq 0.5$ at. % the dominant defects

would be *A* centers. However, for concentrations of $\simeq 6$ at. %, other kind of defects, possibly *DX* centers, appear to be more numerous. These results suggest that while *A* centers become a limiting factor in carrier passivation, for higher In concentrations *DX* centers would control the incorporation of carriers, explaining the observation of phenomena such as persistent photoconductivity and persistent paramagnetic resonace in this system.

*Present address: Centro de Investigacion de Ciencia Aplicada y Tecnologia Avanzada del Instituto Politecnico Nacional, Mexico D.F. 11500, Mexico.

[1] For a review of the case of II-VI semiconductors see U.V. Desnica, Prog. Cryst. Growth Charact. Mater. **36**, 291 (1998).

[2] C.H. Park and D.J. Chadi, Phys. Rev. B **52**, 11 884 (1995).

[3] C.H. Park and D.J. Chadi, Phys. Rev. Lett. **75**, 1134 (1995).

[4] E.R. Weber, K. Khachaturyan, M. Hoinkis, and M. Kaminska, in *Point and Extended Defects in Semiconductors*, Vol. 202 of *NATO Advanced Studies Institute, Series B:Physics*, edited by G. Benedek, A, Cavallini, and W. Schroter (Institute of Physics, Bristol, 1989), p. 39.

[5] D.J. Chadi, P.H. Citrin, C.H. Park, D.L. Adler, M.A. Marcus, and H.J. Gossmann, Phys. Rev. Lett. **79**, 4834 (1997).

[6] M. Zapata-Torres, R. Castro Rodriguez, A. Zapata-Navarro, F.J. Espinosa, J. Mustre de Leon, and J.L. Peña, Rev. Mex. Fis. **43**, 429 (1997).

[7] J. Petruzello, J. Gaines, P. Van der Sluis, D. Olego, and C. Ponzoni, Appl. Phys. Lett. **62**, 1496 (1993).

[8] F.J. Espinosa, J. Mustre de Leon, M. Zapata-Torres, R. Castro-Rodriguez, J.L. Peña, S.D. Conradson, and N.J. Hess, Phys. Rev. B **55**, 7629 (1997).

[9] F.J. Espinosa, J. Mustre de Leon, and I. Hernandez-Calderon, Rev. Mex. Fis. **45S1**, 167 (1999).

[10] K. Khachaturyan, M. Kaminska, E.R. Weber, P. Becla, and R.A. Street, Phys. Rev. B **40**, 6304 (1989).

[11] T.N. Theis, P.M. Mooney, and B.D. Parker, J. Electron. Mater. **20**, 35 (1990).

[12] J. Han, M.D. Ringle, Y. Fan, and R.L. Gunshor, Appl. Phys. Lett. **65**, 3230 (1994).

[13] T. Thio, J.W. Bennet, and P. Becla, Phys. Rev. B **54**, 1754 (1996).

[14] G.W. Iseler, J.A. Kalafas, A.J. Strauss, H.F. MacMillan, and R.H. Bubbe, Solid State Commun. **10**, 619 (1972).

[15] A. Erbil, W. Weber, G.S. Cargill, and R.F. Boehme, Phys. Rev. B **34**, 1392 (1986).

[16] F. Sette, S.J. Pearton, J.M. Poate, J.E. Rowe, and J. Stohr, Phys. Rev. Lett. **56**, 2637 (1986)

[17] P.A. Lee, P.H. Citrin, P. Eisenberger, and B.M. Kincaid, Rev. Mod. Phys. **53**, 769 (1981).

[18] T.C. Anthony, A.L. Fahrenbruch, and R.H. Bubbe, J. Vac. Sci. Technol. A **2**, 1326 (1984).

[19] R. Castro-Rodriguez and J.L. Peña, J. Vac. Sci. Technol. A **11**, 730 (1993).

[20] J. Mustre de Leon, J.J. Rehr, S.I. Zabinski, and R.C. Albers, Phys. Rev. B **44**, 4146 (1991); J.J. Rehr, J. Mustre de Leon, S.I. Zabinski, and R.C. Albers, J. Am. Chem. Soc. **113**, 5135 (1991).

[21] T.A. Tyson, J. Mustre de Leon, S.D. Conradson, A.R. Bishop, J.J. Neumeier, and J. Zang, Phys. Rev. B **53**, 13 985 (1996).

[22] S. Merce, *Standard X-ray Diffraction Powder Patterns*, Natl. Bur. Stand. (U.S.) Monograph No. 25 (U.S. GPO, Washington, D.C., 1964), p. 321.

[23] Following Vegard's rule, if we allow one of these vacancies per In atom, the lattice parameter would be $a = 5.87(x) + 6.48(1 - x)$ with *x* being the concentration of *A* centers. This reproduces the observed decrease in the lattice parameter given in Ref. 8.

[24] A.L. Ankudinov, B. Ravel, J.J. Rehr, and S.D. Conradson, Phys. Rev. B **58**, 7565 (1998).

[25] F.J. Espinosa, J. Mustre de Leon, S.D. Conradson, M. Zapata-Torres, and J.L. Peña, Phys. Rev. Lett. **86**, 3446 (1999).